

High-gain Wideband Fabry-Perot Resonator Antenna Based on Single-layer FSS Structure

Zhiming Liu, Shaobin Liu*, Xiangkun Kong, Zhengyu Huang, and Xing Zhao

College of Electronic and Information Engineering

Nanjing University of Aeronautics and Astronautics, NUAA, Nanjing, 211106, P.R. China

lzmedu@foxmail.com, *lsb@nuaa.edu.cn, xkkong@nuaa.edu.cn, huangzyjn@nuaa.edu.cn, elezhaoxg@163.com

Abstract — In this paper, a wideband Fabry-Perot (FP) resonator antenna is designed based on single-layer frequency selective surface (FSS) structure. The antenna adopts a single-layer complementary circular FSS structure as the partially reflecting surface (PRS) of Fabry-Perot resonator antenna to improve the gain. The wideband slot-coupled patch antenna is used as the source. The proposed FSS maintains a positive slope reflection phase gradient in the band of 10.3-16.0 GHz, which satisfies the realization conditions of the wideband Fabry-Perot resonator antenna. The measured results show that the 10-dB impedance matching bandwidth of the proposed Fabry-Perot resonator antenna covers 11.99-15.54 GHz (25.8%), the maximum gain is 13.16 dBi at 14.2 GHz, and the 3-dB gain bandwidth is 26.1%. The measurement results verify the feasibility of the design method.

Index Terms — Fabry-Perot resonator antenna, frequency selective surface, high-gain, wideband antenna.

I. INTRODUCTION

The Fabry-Perot resonator antenna is composed of a source antenna and a PRS. The Fabry-Perot antenna has the characteristics of high gain, high orientation, low profile and easy processing [1-5]. In recent years, many researchers have been attracted by the excellent performances of FP resonant cavity antenna [6-10].

In general, the reflection phase of the PRS has the characteristic of high Q value. Therefore, the gain enhancement of the FP resonator antenna is narrow-band. In order to improve the operating bandwidth of the FP resonator antenna, the PRS with the gradient structure can be used to compensate the phase in the different propagation direction, thus the PRS structure with gain enhancement in a wide band for FP resonator antenna. In [11], a single-layer FSS with quasi-periodic gradient is used as the PRS of the FP resonator antenna. The FSS structure with gradual change from the middle to the outer side can compensate the radiation phase appropriately, and the broadband FP resonator antenna with the maximum gain of 18.53 dBi and 3-dB gain

bandwidth (GB) of 12.2% is realized. In [12], it applies this idea to the ground of the radiation source, and increases the gain bandwidth of the FP resonator antenna by loading the high impedance surface (HIS) on the metal ground.

In addition, the multi-layer PRS structure can also achieve bandwidth gain enhancement. In [13], a two-layer periodic structure is used as PRS of FP resonator antenna, and a broadband FP resonator antenna with a relative bandwidth of 5.1% and the maximum gain of 17.44 dBi is obtained. In [14], a multi-layer broadband FP resonator antenna fed with double slot coupling is proposed, the broadband FP resonator antenna with the fractional bandwidth of 16% and the maximum gain of 19 dBi is realized. In [15], through the exquisite design of three layer PRSs, a broadband FP resonator antenna with multi-layer PRS has the relative bandwidth of 10.7%, and it has the maximum gain of 16.9dBi. Although the FP resonator antenna with multi-layer PRS has large gain, its profile is large and its relative bandwidth is narrow.

In recent years, the PRS with positive reflection phase gradient has attracted the attention of scholars for improving the gain bandwidth of FP resonator antenna. In [16], two layers of dielectric superstrates with positive slope reflection phase gradient is used as PRS. The wideband FP resonator antenna with the relative bandwidth of 25.8% and the maximum gain of 15 dBi is realized. The antenna has good properties, but it has a high profile. In [17], a broadband FP resonator antenna with the relative bandwidth of 15% and the maximum gain of 20 dBi is proposed by using three layers periodic PRSs with positive reflection phase gradient. The FP resonator antenna formed by PRS with positive reflection phase gradient can effectively improve its 3-dB gain bandwidth, but its profile is high.

In order to expand the 3-dB gain bandwidth and reduce profile of the FP resonator antenna, a FSS with circular complementary structure is etched on both sides of the substrate as the PRS to form the FP resonator antenna in this paper. The FSS with positive reflection phase gradient in the band of 10.3-16.0 GHz, and a slot-

coupled patch antenna as the source to achieve a wideband FP resonator antenna. The measured results show that the proposed antenna with $|S_{11}| < -10$ dB of 11.99-15.54 GHz, the 3-dB gain bandwidth of 12.36-15.6 GHz, and the peak gain of 13.16 dBi.

II. FSS AND RADIATION ANTENNA

A. Numerical analysis

As shown in Fig. 1, the FP resonator is actually a semi-open resonator, which consists of a ground and a partially reflecting surface. The electromagnetic wave radiated by the source is reflected repeatedly between the upper and lower surfaces of the resonant cavity. Assuming that the incident wave with frequency of f illuminates the ground and the metal ground has total reflection properties, the reflection amplitude of ground is equal to 1. Therefore, the reflection coefficient of ground can be expressed as $e^{j\varphi_{GND}}$, where φ_{GND} is the reflection phase of ground. Meanwhile, the reflection coefficient of PRS can be expressed as $pe^{j\varphi_{PRS}}$, where p and φ_{PRS} denote reflection amplitude and reflection phase of the PRS, respectively. Considering that the source is much smaller than the overall size of the Fabry-Perot resonator, it can be approximately regarded as a point source.

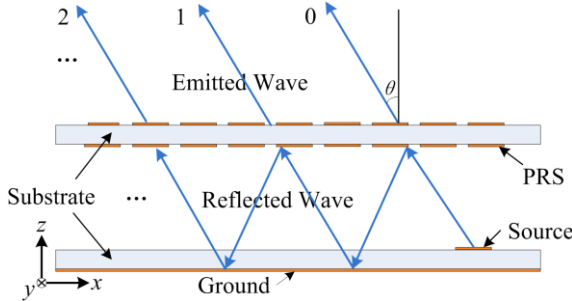


Fig. 1. The schematic diagram of Fabry-Perot resonator.

The electric field intensity of each electromagnetic wave transmitted from PRS is superimposed as [1]:

$$E = \sum_{n=0}^{\infty} f(\alpha) E_0 p^n \sqrt{1-p^2} e^{j\Theta_n}, \quad (1)$$

$$\Theta_n = n\Phi = n\left(-\frac{4\pi f}{c} h \cos \alpha + \varphi_{GND} + \varphi_{PRS}\right), \quad (2)$$

where E_0 is the amplitude of the first emitted wave, Θ_n is the total phase variations during the reflections between the ground and the PRS, n denotes the n th emitted wave, $f(\alpha)$ is the field intensity direction function, α is the incidence angle, c is the velocity of light, h is the thickness of cavity. The absolute value of field strength is expressed as:

$$|E| = |E_0| f(\alpha) \sqrt{\frac{1-p^2}{1+p^2-2p\cos\Phi}}. \quad (3)$$

Thus, the power pattern S is:

$$S = \frac{1-p^2}{1+p^2-2p\cos(\varphi_{GND} + \varphi_{PRS} - \frac{4\pi f}{c} h \cos \alpha)} f^2(\alpha), \quad (4)$$

when $\alpha=0^\circ$, the power pattern S becomes:

$$S = \frac{1-p^2}{1+p^2-2p\cos(\varphi_{GND} + \varphi_{PRS} - \frac{4\pi f}{c} h)} f^2(0). \quad (5)$$

The maximum power in the direction of $\alpha=0^\circ$ can be obtained when:

$$\varphi_{GND} + \varphi_{PRS} - \frac{4\pi f}{c} h = 2n\pi, \quad n=0,1,2,\dots, \quad (6)$$

and the maximum power pattern is:

$$S_{max} = \frac{1+p}{1-p} f^2(0). \quad (7)$$

It can be concluded that when f , h , φ_{GND} and φ_{PRS} satisfy the resonance condition of equation (6), the FP resonator antenna will have the largest forward energy density. From equation (7), the power pattern S of FP resonator antenna is positively correlated with the reflection amplitude of the PRS, which means that as the p increases, the maximum power pattern S_{max} of the FP resonator antenna will increase.

Assuming that the directivity of the source antenna is D_0 at frequency f , and the directivity is D_s after adding a PRS above it. By equation (7), the relative directivity D can be expressed as follows:

$$D(\text{dB}) = 10 \log_{10} \left(\frac{1+p}{1-p} \right). \quad (8)$$

According to the above numerical analysis, as the f , h , φ_{GND} and φ_{PRS} satisfy the Fabry-Perot resonance condition, the FP resonance mode can be excited. The directivity of FP resonator antenna is positively correlated with the reflection amplitude of PRS. In order to obtain a large directivity of the FP resonator antenna, the reflection amplitude of the designed PRS should be as large as possible.

B. The design of FSS

From equation (6), the PRS reflection phase can be expressed as:

$$\varphi_{PRS} = \frac{4\pi h}{c} f + 2N\pi - \varphi_{GND}, \quad (9)$$

where h is the thickness of the cavity, c is the velocity of light, and φ_{PRS} is the reflection phase of PRS, $\varphi_{GND} = -\pi$. It can be seen that when the resonant cavity height h , resonant frequency f and φ_{PRS} meet the equation (9), the FP resonance mode can be excited to achieve the gain enhancement. Therefore, the PRS with positive reflection phase gradient is the key point to design the wideband FP resonator antenna.

The design of PRS structure is an important part for the wideband FP resonator antenna. In this paper, the

designed FSS acts as PRS, the proposed FSS structure is shown as shown in Fig. 2 (a). The FSS unit is composed of a circular complementary structure, $p=6.5$ mm, it is etched on both sides of the F_4BM220 substrate with the thickness of 1.5 mm ($\epsilon_1=2.2$, $\tan\delta=0.0007$).

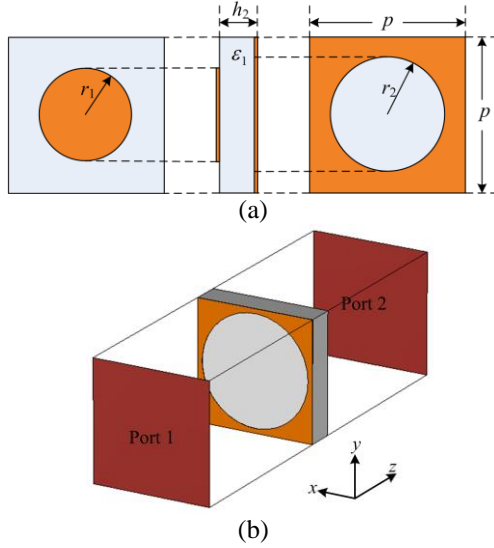


Fig. 2. The unit of FSS: (a) structure and (b) simulation model.

To analyze the characteristic of positive reflection phase gradient of FSS structure, the parameters of FSS are analyzed. Fig. 2 (b) is the schematic diagram of simulation model. Port 1 and Port 2 are set at a distance from the FSS unit, and the boundary conditions of the simulation models are set to magnetic boundary and electrical boundary in the direction of $\pm x$ and $\pm y$, respectively. When the incident wave propagates along the $+z$ direction, the simulated results of parameters scanning are shown in Fig. 3. In Fig. 3 (a), fixed $r_2=3.0$ mm, with the increase of r_1 , the resonance frequency shifts to low frequency, the reflection amplitude increases slightly, the slope of the reflection phase curve is approximately the same, and the positive reflection phase gradient bands shift to the low frequency. In Fig. 3 (b), fixed $r_1=2.3$ mm, with the increase of r_2 , the resonance frequency shifts to low frequency, the reflection amplitude decreases obviously, the slope of the reflection phase curve increases, and the positive reflection phase gradient bands also shift to low frequency. Select parameters $h_2=1.5$ mm, $r_1=2.3$ mm, $r_2=3$ mm, the FSS unit structure has a positive slope reflection phase gradient band in the range of 10.3-15.9 GHz, and the reflection amplitude is more than 0.58. According to the equation (9), it is known that the FP resonator antenna designed by the FSS structure can excite the FP resonance mode in a wide band, and realize the gain enhancement of the FP resonator antenna in a wide band.

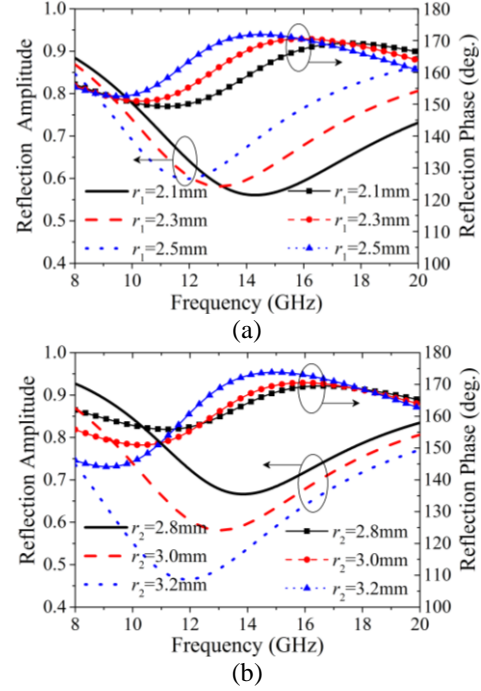


Fig. 3. The reflection coefficients of PRS: (a) $r_2=3.0$ mm and (b) $r_1=2.3$ mm.

C. Source antenna

The designed wideband source antenna is made up of a slot antenna and parasitic patch, as shown in Fig. 4. The ground and feed line of the slot antenna are etched on both sides of the F_4BM220 substrate ($\epsilon_2=2.2$, $\tan\delta=0.0007$) with the thickness of 0.8 mm, respectively. The length and width of the slot antenna are $W=60$ mm, and the parasitic patch is placed at $h_{air}=3$ mm above the slot of the ground. The structural parameters are shown in Table 1. As shown in Fig. 5, the $|S_{11}|<-10$ dB of the slot-coupled patch antenna is 12.36-16.29 GHz, and the maximum gain is 8.33 dBi at 15.0 GHz. Apparently, the 10-dB impedance matching bandwidth of the source antenna is within the range of the positive slope reflection phase gradient band of the designed FSS.

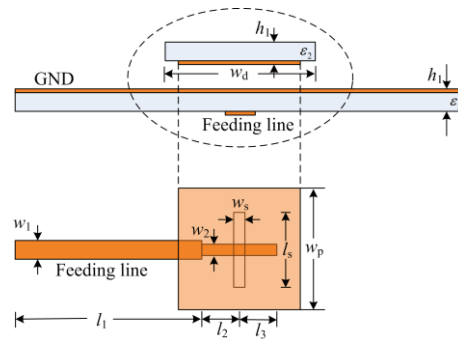


Fig. 4. The schematic diagram of the slot-coupled patch antenna.

Table 1: Parameters value of the slot-coupled patch antenna

Parameters	h_1	l_1	l_2	l_3	l_s
Value (mm)	0.8	24	6	1.7	7
Parameters	w_p	w_d	w_1	w_2	w_s
Value (mm)	5.5	10	2.3	0.9	1

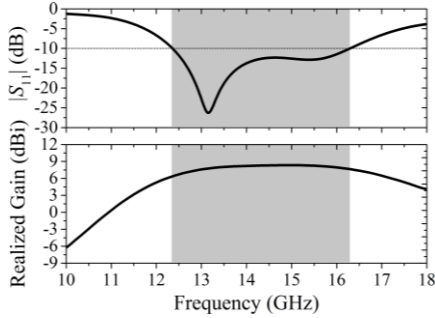


Fig. 5. The simulated results of the slot-coupled patch antenna.

III. WIDEBAND FABRY-PEROT ANTENNA

A. Wideband Fabry-Perot antenna

Based on the above design of the FSS structure and the source, an FP resonator antenna with wideband and high gain is designed. The unit of FSS element is etched in a 7×7 periodicity on the F_4BM220 substrate of $W \times W$, and placed at h_c above the ground of slot antenna. Figure 6 is the schematic diagram of the wideband FP resonator antenna. A part of the electromagnetic wave radiated by slot-coupled patch antenna is reflected in the cavity, and part of it is transmitted through the FSS structure. When the thickness of the cavity and the reflection phase of the FSS satisfy the FP resonance condition, the gain is enhanced.

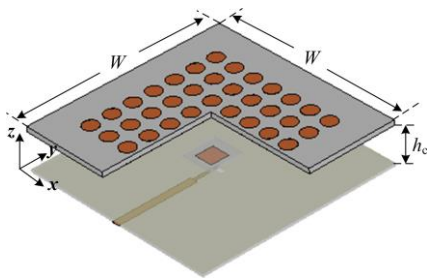


Fig. 6. The schematic diagram of the proposed antenna.

The thickness of FP cavity is an important factor that affects the performance of wideband FP resonator antenna. In order to design FP resonator antenna with good performance, the influence of different cavity thickness on the bandwidth and gain of FP resonator antenna should be taken into account.

The effect of different cavity thickness on the $|S_{11}|$ and the realized gain of FP resonator antenna is analyzed. As shown in Fig. 7 and Table 2, other parameters are fixed, as the h_c increases from 9.5 mm to 11.0 mm by step length 0.5 mm, the $|S_{11}| < -10$ dB of the designed antenna is changed from two to one, and the relative bandwidth is gradually expanded, while the 3-dB gain bandwidth is increased first and then reduced, but the maximum gain is gradually reduced. Therefore, considering the design of the wideband FP resonator antenna with large operating bandwidth and high gain, $h_c = 10.5$ mm is selected. For this case, the proposed antenna with the 10-dB impedance matching bandwidth of 11.99-15.81 GHz (27.4%), 3-dB gain bandwidth of 11.9-15.5 GHz (26.3%), and the maximum gain of 13.26 dBi at 15.0 GHz. Meanwhile, the half-power beamwidth of 15.0 GHz of the E- and H- planes are 23.9° and 39.2° , respectively.

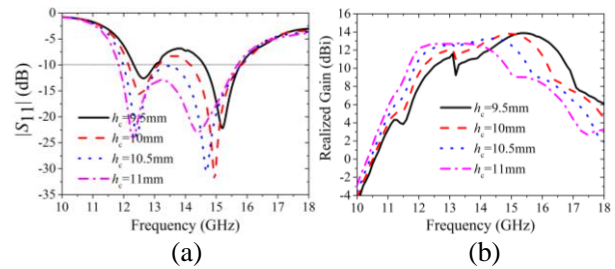
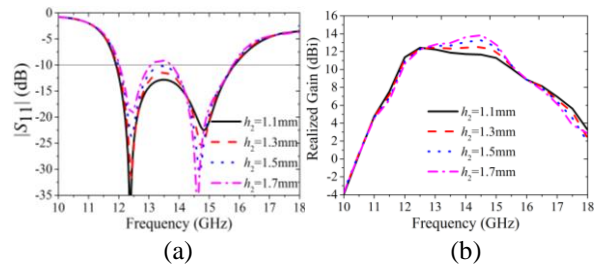

 Fig. 7. The simulated results of vary h_c : (a) S_{11} and (b) realized gain.

 Table 2: Comparison between different h_c

h_c (mm)	$ S_{11} < -10$ dB (GHz)	3-dB Gain Bandwidth (GHz)
9.5	12.32-13.02 (5.5%) 14.60-15.79 (7.8%)	13.6-16.7 (20.5%)
10.0	12.15-13.12 (7.7%) 14.16-15.82 (11.1%)	12.3-16.1 (26.8%)
10.5	11.99-15.81 (27.4%)	11.9-15.5 (26.3%)
11.0	11.84-15.68 (27.9%)	11.7-14.9 (24.1%)


 Fig. 8. The simulated results of proposed antenna with different h_2 : (a) $|S_{11}|$ and (b) realized gain.

The effect of h_2 on the performance of the proposed antenna is also considered. We fixed other parameters and scan the h_2 from 1.1 mm to 1.7 mm by step of 0.2 mm. The simulated results are shown in Fig. 8. It shows that when h_2 increases from 1.1 mm to 1.5 mm, the 10-dB impedance matching bandwidth of the proposed antenna remains the same basically, while as $h_2 = 1.7$ mm, the antenna has two operating bands with 10-dB impedance matching level. In addition, the maximum realized gain of the proposed antenna enhances with the increase of h_2 . Therefore, to ensure the high performance of the proposed antenna, $h_2 = 1.5$ mm is selected.

B. Experiments

The designed wideband FP resonator antenna is fabricated, and its experiment is completed in the microwave anechoic chamber. The measurement scene is shown in Fig. 9.

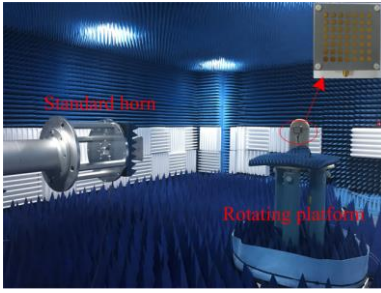


Fig. 9. The measurement scene of the proposed antenna.

Figure 10 shows that the measured and simulated results of the $|S_{11}|$ and realized gain of the proposed antenna. In Fig. 10, the measured results show that the impedance bandwidth $|S_{11}| < -10$ dB of the source antenna is 12.61-16.19 GHz, and the maximum gain is 8.18 dBi at 15.4 GHz. Meanwhile, the measured results show that the impedance bandwidth $|S_{11}| < -10$ dB of the proposed wideband FP resonator antenna is 11.99-15.54 GHz (25.8%), the 3-dB gain bandwidth is 12.36-15.6 GHz (26.1%), and the maximum gain value is 13.16 dBi at 14.2 GHz, it is approximately consistent with the simulated results.

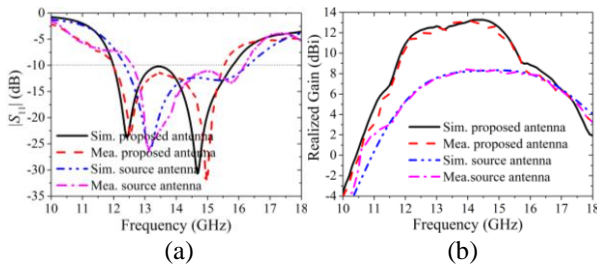


Fig. 10. The comparisons of measured and simulated results: (a) S_{11} and (b) realized gain.

Also, the simulated and measured radiation patterns of the proposed antenna at 12.5 GHz, 13.5 GHz, 14.5 GHz and 15.5 GHz, respectively, in both planes are shown in Fig. 11. It can be observed that the designed antenna has good radiation pattern in the operating band. Finally, the proposed antenna is compared with the existing similar work in Table 3. It shows that the proposed antenna has a lower profile, wider operating bandwidth and the 3-dB gain bandwidth is extended.

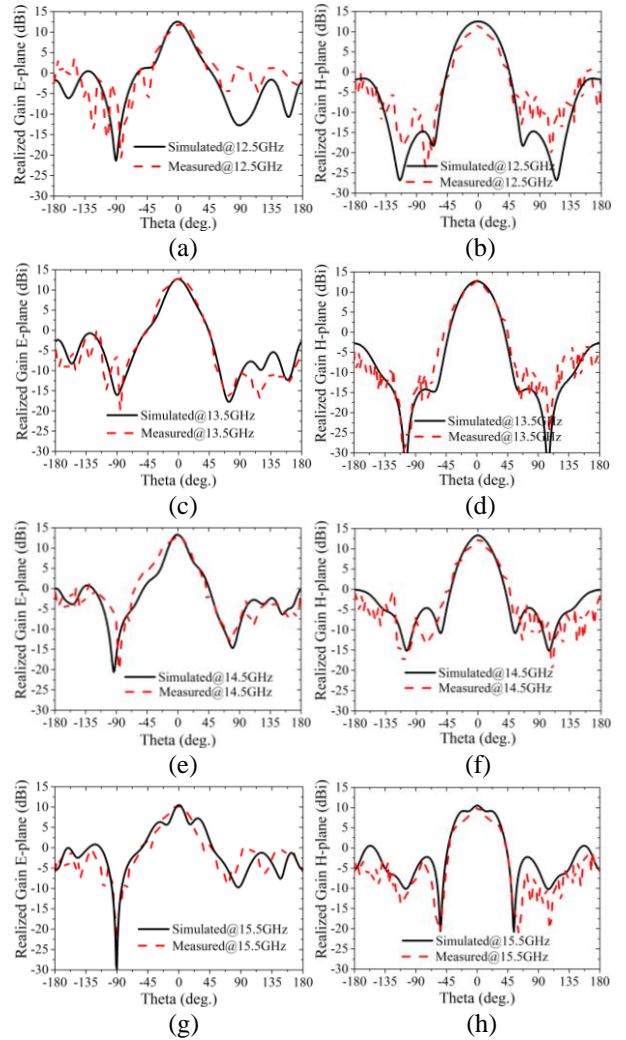


Fig. 11. The radiation patterns of the proposed antenna: (a) E-plane, (b) H-plane at 12.5 GHz, (c) E-plane, (d) H-plane at 13.5 GHz, (e) E-plane, (f) H-plane at 14.5 GHz, and (g) E-plane, (h) H-plane at 15.5 GHz.

IV. CONCLUSION

A wideband high-gain Fabry-Perot resonator antenna is designed based on single-layer FSS structure. The wideband slot-coupled patch antenna is used as the source antenna, the FSS with circular complementary structure is used as the PRS. Moreover, the influence

of various parameters on the antenna performance is analyzed. The measured results show that the proposed antenna has the 10-dB impedance matching bandwidth of 11.99-15.54 GHz (25.8%), the 3-dB gain bandwidth of 12.0-15.6 GHz (26.1%), and the maximum gain value of 13.16 dBi at 14.2 GHz, it confirms the correctness of the simulated results.

Table 3: Comparison between the designed antenna and the existed work

Ref.	$ S_{11} < -10$ dB (GHz)	3-dB GB	Height (mm)	Max. Gain (dBi)	Aperture (mm ²)	PRS Num.
[13]	13.4– 14.1	5.1%	23.4	17.44	280×280	2
[15]	13–14.5	10.9%	16.44	15	80×80	3
[16]	13.6– 18.4	25.8%	26.3	15	45×45	2
[17]	13.5– 15.7	15%	35	20.0	80×80	3
This work	11.99– 15.54	26.1%	12.8	13.16	60×60	1

ACKNOWLEDGMENT

This work was supported by Chinese Natural Science Foundation (Grant No. 61671238; No. 61471368), the Fundamental Research Funds for the Central Universities (No. NJ20160008; NS2017026), Project Funded by China Postdoctoral Science Foundation (Grant No. 2016M601802), Jiangsu Planned Projects for Postdoctoral Research Funds (Grant No. 1601009B), Aeronautical Science Foundation of China (20161852016), and the Funding of Jiangsu Innovation Program for Graduate Education (No. KYLX16_0371), the Fundamental Research Funds for the Central Universities.

REFERENCES

- [1] G. V. Trentini, "Partially reflecting sheet arrays," *IRE Trans. Antennas Propag.*, vol. 4, no. 4, pp. 666-671, 1956.
- [2] S. Bibi, R. Saleem, A. Quddus, and M. F. Shafique, "Dual-band antenna for high gain M2M communication using PRS," *Applied Computational Electromag. Soc. J.*, vol. 32, no. 11, pp. 994-1000, 2017.
- [3] Z. Liu, S. Liu, B. Bian, X. Kong, and H. Zhang, "Metasurface-based low-profile high-gain substrate-integrated Fabry-Pérot cavity antenna," *Int. J. RF Microw. Comput. Aided Eng.*, p. e21583, 2018.
- [4] W. Liu, Z. N. Chen, T. S. P. See, and F. Liu, "SIW-slot-fed thin beam-squint-free Fabry-Pérot cavity antenna with low backlobe levels," *IEEE Antennas Wirel. Propag. Lett.*, vol. 13, pp. 552-554, 2014.
- [5] Y. Zhang, W. Yu, and W. Li, "Study on Fabry-Pérot antennas using dipole exciters," *Applied Computational Electromag. Soc. J.*, vol. 29, no. 12, pp. 1112-1116, 2014.
- [6] H. H. Tran and T. K. Nguyen, "K-band planar and low-profile Fabry-Perot cavity antenna with a coupled strip-slitline feed structure," *Applied Computational Electromag. Soc. J.*, vol. 32, no. 6, pp. 542-547, 2017.
- [7] Z. G. Liu, Z. X. Cao, and L. N. Wu, "Compact low-profile circularly polarized Fabry-Perot resonator antenna fed by linearly polarized microstrip patch," *IEEE Antennas Wirel. Propag. Lett.*, vol. 15, pp. 524-527, 2016.
- [8] Y. F. Cheng, W. Shao, X. Ding, and M. X. Yu, "Design of tilted-beam Fabry-Perot antenna with aperiodic partially reflective surface," *Applied Computational Electromag. Soc. J.*, vol. 32, no. 5, pp. 397-404, 2017.
- [9] P. Liu, J. Chen, and Y. Hu, "Accelerated storage testing and life assessment method of antenna," *Equip. Environ. Eng.*, vol. 15, no. 3, pp. 98-102, 2018.
- [10] Y. Zheng, J. Gao, Y. Zhou, X. Cao, H. Yang, S. Li, and T. Li, "Wideband gain enhancement and RCS reduction of Fabry-Perot resonator antenna with chessboard arranged metamaterial superstrate," *IEEE Trans. Antennas Propag.*, vol. 66, no. 2, pp. 590-599, 2018.
- [11] Z. Liu, W. Zhang, D. Fu, Y. Gu, and Z. Ge, "Broadband Fabry-Perot resonator printed antennas using FSS superstrate with dissimilar size," *Microw. Opt. Technol. Lett.*, vol. 50, no. 6, pp. 1623-1627, 2008.
- [12] Z. H. Wu and W. X. Zhang, "Broadband printed compound air-fed array antennas," *IEEE Antennas Wirel. Propag. Lett.*, vol. 9, pp. 187-190, 2010.
- [13] C. Mateo-Segura, A. P. Feresidis, and G. Goussetis, "Bandwidth enhancement of 2-D leaky-wave antennas with double-layer periodic surfaces," *IEEE Trans. Antennas Propag.*, vol. 62, no. 2, pp. 586-593, 2014.
- [14] K. Konstantinidis, A. P. Feresidis, and P. S. Hall, "Dual-slot feeding technique for broadband Fabry-Perot cavity antennas," *IET Microw. Antennas Propag.*, vol. 9, no. 9, pp. 861-866, 2015.
- [15] K. Konstantinidis, A. P. Feresidis, and P. S. Hall, "Broadband sub-wavelength profile high-gain antennas based on multi-layer metasurfaces," *IEEE Trans. Antennas Propag.*, vol. 63, no. 1, pp. 423-427, 2015.
- [16] N. Wang, J. Li, G. Wei, L. Talbi, Q. Zeng, and J. Xu, "Wideband Fabry-Perot resonator antenna with two layers of dielectric superstrates," *IEEE Antennas Wirel. Propag. Lett.*, vol. 14, pp. 229-232, 2015.

- [17] K. Konstantinidis, A. P. Feresidis, and P. S. Hall, "Multilayer partially reflective surfaces for broadband Fabry-Perot cavity antennas," *IEEE Trans. Antennas Propag.*, vol. 62, no. 7, pp. 3474-3481, 2014.



Zhiming Liu was born in Jiangxi Province, China, in 1989. He received the B.S. degree and M.S. degree from East China Institute of Technology, Fuzhou, China, in 2012 and Nanchang University, Nanchang, China, in 2015, respectively. He is currently pursuing the Ph.D. degree

in College of Electronic and Information Engineering, Nanjing University of Aeronautics and Astronautics, Nanjing, China. His research interests include Antennas and Metasurface.



Shaobin Liu received the Ph.D. degree in Electronics Science and Technology from the National University of Defense Technology in 2004. However, in 2003, he was already promoted as Professor. He is currently a Professor of Electromagnetic and Microwave Technology at the Nanjing University of Aeronautics and Astronautics. His research focuses on plasma stealthy antennas, microwave, radio frequency, electromagnetic compatibility.



Xiangkun Kong received the Ph.D. degree in Communication and Information Systems from the Nanjing University of Aeronautics and Astronautics (NUAA) in 2015. He has been an Associate Professor in NUAA, since his promotion in July 2015. He used to work at the

University of St. Andrews in the UK as an Academic Visitor supported by China Scholarship Council. His main research interests include the plasma stealth, plasma photonic crystal, electromagnetic properties of metamaterials, and computational electromagnetics. He has published more than 60 papers in different academic journals, including *Applied Physics Letters*, *Optics Express*, and *IEEE Journal of Selected Topics in Quantum Electronics*, and has been cited 1099 times.



Zhengyu Huang was born in Hunan, China, in 1986. He received the B.S. degrees in Electronic and Information Engineering from Nanchang University, Nanchang, China, in 2008 and the Ph.D. degree in Electromagnetic Environmental Effects and Electro-optical Engineering from

PLA University of Science and Technology, Nanjing, China, in 2016. He has co-authored one monograph on the Associated Hermite finite-difference time-domain method and 30 peer-reviewed journal papers included in the Web of Science Core Collection. He was the recipient of the Outstanding Doctoral Dissertation Award of the PLA University of Science and Technology in 2017 and the Excellent Doctoral Dissertation Award by Lu Zhitao Academician in 2018.

He is currently an Associate Professor with Key Laboratory of Radar Imaging and Microwave Photonics, Nanjing University of Aeronautics and Astronautics, Nanjing, China. His research interests include computational electromagnetics, electromagnetic compatibility and multiphysics modeling and analysis.



Xing Zhao was raised in Tianjin, China. He received the B.Eng. degree in Information Engineering from Shanghai Jiao Tong University, Shanghai, China, in 2008, and the M.S. and Ph.D. degrees in Electronics and Computer Engineering from Hanyang University, Seoul, South Korea, in

2010 and 2014, respectively.

From 2015 to 2017, he was a Postdoctoral Research Fellow with the Department of Electrical and Computer Engineering, National University of Singapore, Singapore. He is currently an Associate Research Fellow with the College of Electronic and Information Engineering, Nanjing University of Aeronautics and Astronautics, China.

His current research interests include small antennas for 5G mobile MIMO platforms and integrated array antennas for radar system.